CHAPTER - IV

PREPARATION AND CHARACTERIZATION OF COPPER OXIDE THIN FILMS

4.1 INTRODUCTION

The transition metal oxides, form a group of predominantly ionic solids, which exhibit a wide range of optical and electrical properties. Many of these oxides have shown outstanding activity for a variety of electrochemical processes of technological interest. Copper oxide is one of the versatile oxide materials among the metal oxides. Copper oxide has been studied as a semiconductor material because of natural abundance of starting material (Cu); low cost production processing; non toxic nature; and reasonably good electrical and optical properties [1]. Several methods have been used to prepare copper oxide thin films. In most of these studies, a mixture of phases, like Cu, CuO and Cu_2O, at room temperature is generally obtained, and this is one of the nagging problems for utilizing Cu_2O as a semiconductor [2-5]. The inability to prepare n-type Cu_2O also restricts its applications to Schottky barrier and heterojunction photovoltaic devices [6-9]. The control of crystallite size in semiconductor thin films within nanometric dimensions is known to modify optical and electrical properties due to quantum confinement and enhanced surface effects. The synthesis of Cu_2O as nanoparticles or nanocrystalline thin films seems to be a possible methodology for stabilizing the cuprous phase and for the realisation of n-type conductivity. This will make nanocrystalline Cu_2O an attractive

semiconductor material for the fabrication of low cost solar cells and other opto-electronic devices [10].

Spray pyrolysis, which is one of the chemical techniques has been applied to deposit a wide variety of films including cupric oxide (CuO). The preparation of different photovoltaic compound thin films for solar cells has been attempted by a spray pyrolysis deposition (SPD) technique using simple apparatus with good productivity. There are several copper oxide film deposition methods. The methods that use oxidation require a copper substrate and those that use electro-deposition require electrically conducting substrates. That is these deposition methods are restricted by the substrate material. Furthermore physical methods require a complicated apparatus that include a high vacuum system.

In the present chapter, an emphasis has been given on the deposition of copper oxide films onto the glass substrates by pneumatic spray pyrolysis technique, using solution of cupric acetate in methanol and study of their structural, optical and electrical properties. Due to simplicity, low cost and feasibility for mass production, the spray pyrolysis technique has been used.

The copper oxide films at variable substrate temperatures were prepared and the effect of substrate temperature and post annealing treatment on structural, electrical and optical properties was studied

using various characterization techniques. Substrate temperature is one of the important parameters, which influences material properties and can be controlled to obtain desired properties suitable for a particular application.

4.2 EXPERIMENTAL PROCEDURE

Copper oxide thin films were obtained by spraying a 0.01 M solution of cupric acetate $(CH_3COO)_2$ Cu, H_2O (molecular weight 199.65 gm) in methanol onto preheated glass substrates. The addition of methanol to the starting solution is expected to increase the wettability of the droplet and act as an oxidizing agent. Because of reduction of the surface tension it helps in improving the homogeneity of the deposited film. The substrate temperature was varied from 250^0C to 350^0C in the interval of 50^0C. the spray rate was kept constant at 6-7 ml/ min. The samples deposited at different substrate temperatures are denoted by C_{250}, C_{300} and C_{350}. The samples were further annealed in air at 500^0C for half an hour. The annealed samples are denoted by C_{A250}, C_{A300} and C_{A350}, where A denotes the annealed samples. The effect of annealing on structural, electrical and optical properties was examined.

Film thickness was determined by using gravimetric (weight difference) method. The X-ray diffractometer (Philips PW-1710) with CuK_α radiation was used for structural studies in the range of angle 2θ

between 0 to 100^0. Infrared (IR) spectrum was recorded using Perkin-Elmer spectrophotometer Model 783 in the spectral range 400 to 4000 cm^{-1}. For IR measurement the pellets were prepared by mixing KBr with copper oxide powder collected by scratching from the glass substrates in the ratio 300:1 and then pressing the powder between two pieces of polished steel.

To determine the band gap energy, optical absorption study was carried out in the wavelength range between 350 to 850 nm, using Hitachi-330 spectrophotometer. DC electrical resistivity measurement was made using a two probe method in the temperature range 300 to 600 K. The thermo-electric force (emf) was measured as a function of temperature in the temperature range of 300 to 450K.

4.3 RESULTS AND DISCUSSION

The methanolic cupric acetate solution (0.01 M) (the preparation procedure is given in Chapter III) section was sprayed onto preheated glass substrates through specially designed glass nozzle. The sprayed droplets undergo solvent evaporation, solute condensation and thermal decomposition thereby resulting in the formation of the copper oxide films. The chemical reaction that took place is given below

$$(CH_3COO)_2\,Cu, H_2O + CH_3OH \xrightarrow[250 - 350^0C]{air} CH_3COOH\uparrow$$

(Cupric acetate) (methanol) (Acetic acid)

$$+ CH_3 - \underset{\displaystyle O}{\overset{\displaystyle \|}{C}} - OCH_3 + CuO + H_2O\uparrow$$

(methyl acetate)

The films were found to be uniform and well adherent to the glass and FTO coated glass substrates. The colour of the film was brownish at about 250^0C and changes to pale brown at higher substrate temperature of the order of 350^0C. Post annealed films were thin and transparent.

The copper oxide film deposition process could be separated into following steps : As droplet leaves the tip of the nozzle and travel towards the heated substrates, it underwent following changes leading to film formation.

1. Ejection of droplets that contain Cu^{2+} and $(CH_3COO)^{2-}$ species; surrounded by the CH_3OH solvent.
2. Evaporation of CH_3OH solvent; thereby reducing diameter of the droplet.
3. Expulsion of acetate species, leaving behind Cu^{2+} species to react with oxygen, released either from decomposition of CH_3OH, $(CH_3COO)_2$ or ambient air.

4. Formation of copper oxide precipitate, which impinge on the heated substrate surface, acquire sufficient thermal energy leading to increase in copper oxide binding and substrate adherence energies.

5. Formation of adherent and uniform films of copper oxide, the phase formation (Cu_2O/CuO) further depends on substrate temperature; the oxidation advances as the temperature increases. Above steps are illustrated in following figure.

4.3.1 DTA/ TGA of Copper Acetate Powder

The DTA/ TGA of powder is shown in figure 4.1. It is seen from the DTA/ TGA analysis of Cupric acetate powder that upto about 150^0C, water molecules evaporate giving rise to an exothermic peak at 150^0C. The abrupt weight loss near 280^0C is due to expulsion of acetate group from the precursor powder and the corresponding endothermic peak is observed. At about 300^0C, the weight loss is stable, indicating no further decomposition of salt and formation of copper oxide (CuO).

4.3.2 Thickness Measurement

Thickness of the films prepared at different substrate temperatures (C_{250} - C_{350}) were measured by using gravimetric method and assuming the bulk density of the material. The film thickness is calculated by using equation 3.1.

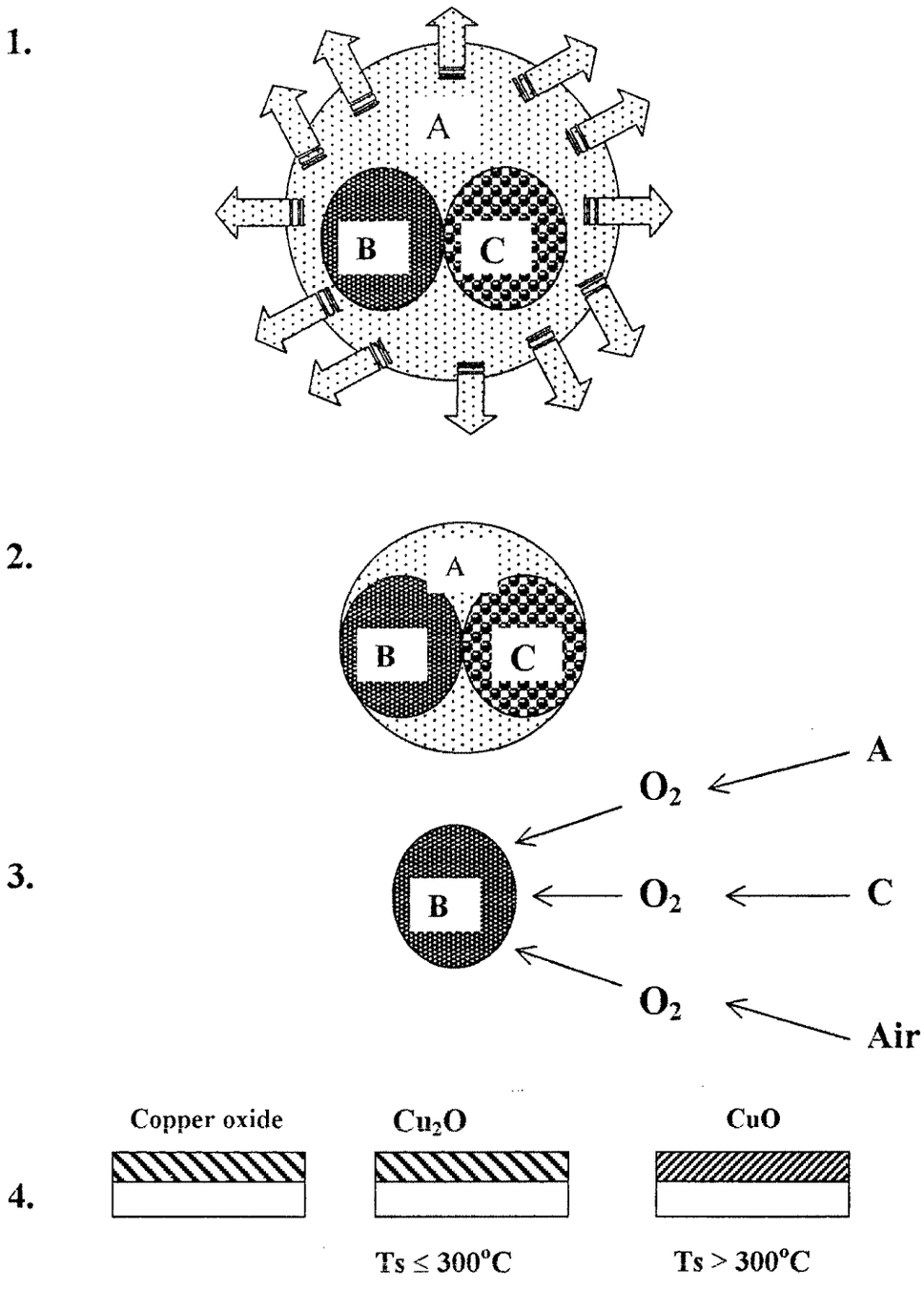

Above figure schematically shows various steps involved in the formation of copper oxide thin films by decomposing droplet. A: Methanol, B: Cu^{+2} species and C: $(CH_3COO)^{2-}$.

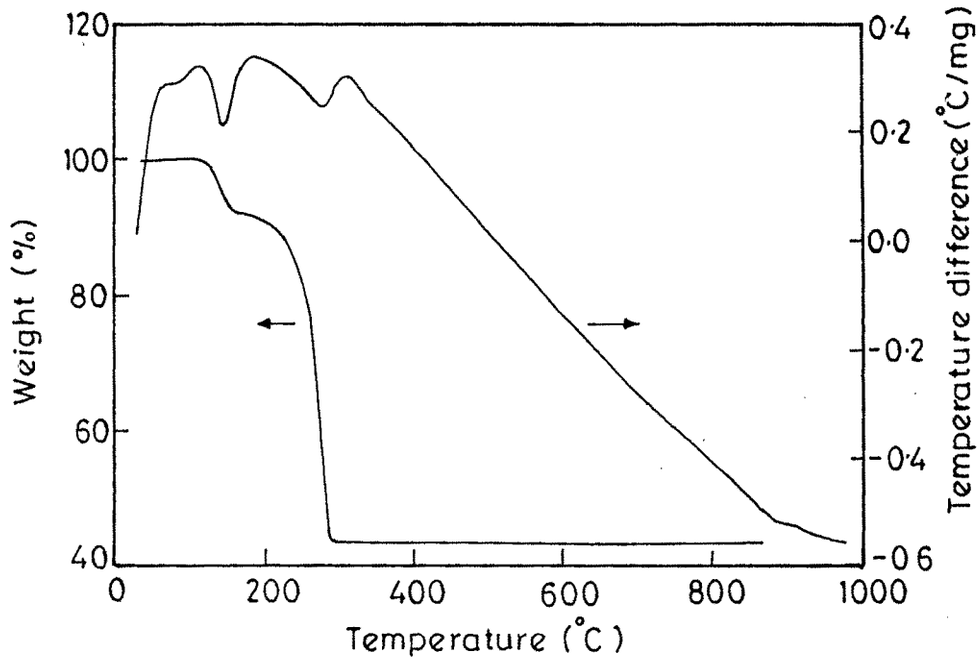

Fig. 4·1 - The DTA-TGA analysis of the copper acetate powder.

The film thicknesses are listed in table 4.1. The variation of film thickness with substrate temperature is shown in Fig. 4.2(a). As substrate temperature increases decrement in film thickness was observed. Similar results have been reported for sprayed oxide and chalcogenide films [11-13]. At higher substrate temperature the radiated upward heat flow may hinder the incident mist flux, which induces a reduction in film thickness. Thickness of the post-annealed films were found to be less than that of the as- deposited films (Fig. 4.2b). The film thicknesses of the post-annealed films (C_{A250} - C_{A350}) are listed in table 4.1.

Table 4.1 : Effect of substrate temperature on properties of copper oxide thin films prepared by spray pyrolysis

Sample	Thickness (μm)	Bandgap Eg (eV)	Electrical resistivity at 300 K (Ωcm)	Activation energy E_a(eV)
C_{250}	0.131	1.87	1.0×10^6	0.30
C_{300}	0.049	1.78	6.0×10^5	0.39
C_{350}	0.045	1.00	1.0×10^4	0.34
C_{A250}	0.129	1.10	2.5×10^5	0.26
C_{A300}	0.047	1.51	2.0×10^5	0.25
C_{A350}	0.043	1.20	8.0×10^3	0.17

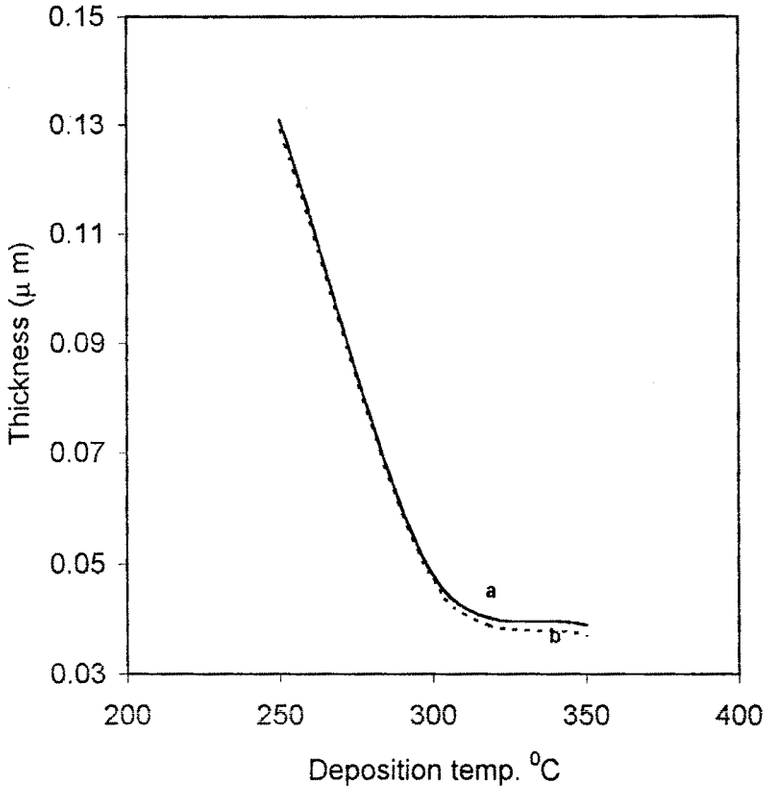

Figure 4.2 Variation of thickness versus deposition temperture.

4.3.3 X-ray Diffraction (XRD) Studies

The structural identification was carried out using X-ray diffraction in the range of angle 2θ between 10^0 and 100^0. Figure 4.3 (a, b, c) shows XRD patterns of copper oxide films (samples C_{250} to C_{350}) prepared at different substrate temperatures. For C_{250} sample a broad hump is seen and no well defined peaks were observed. This is the identification of its amorphicity, nevertheless for C_{250} sample, a minor peak was observed at $2\theta = 38^0$ which corresponds to (101) plane of Cu_4O_3 phase. For sample C_{300}, one peak at $2\theta = 36.870$ was obtained corresponding to Cu_2O phase whereas the sample C_{350} exhibited some minor diffraction peaks corresponding to planes (112) at $2\theta = 51.510$, (021) at $2\theta = 54.640$, (221) at $2\theta = 68.870$ and (222) at $2\theta = 82.940$, indicating the formation of CuO phase. The data of XRD studies of copper oxide thin films by various deposition methods is referred and reported phase changes recorded in the corresponding studies are listed in table 4.2.

Table 4.2 : The copper oxide phases as a function of preparation methods

Preparation method	Copper oxide phase	Reference
Spray pyrolysis	Cu_2O, CuO	[14]
Reactive sputtering	Cu_2O, Cu	[15]
Activated reactive sputtering	Cu_2O	[10]
Chemical vapour deposition	Cu_2O + CuO	[16]
Thermal oxidation	CuO, Cu_2O	[17,18]
Chemical oxidation	CuO, Cu_2O	[17,18]
Electrochemical oxidation	CuO, Cu_2O	[17,18]
Anodic oxidation	CuO, Cu_2O	[19]

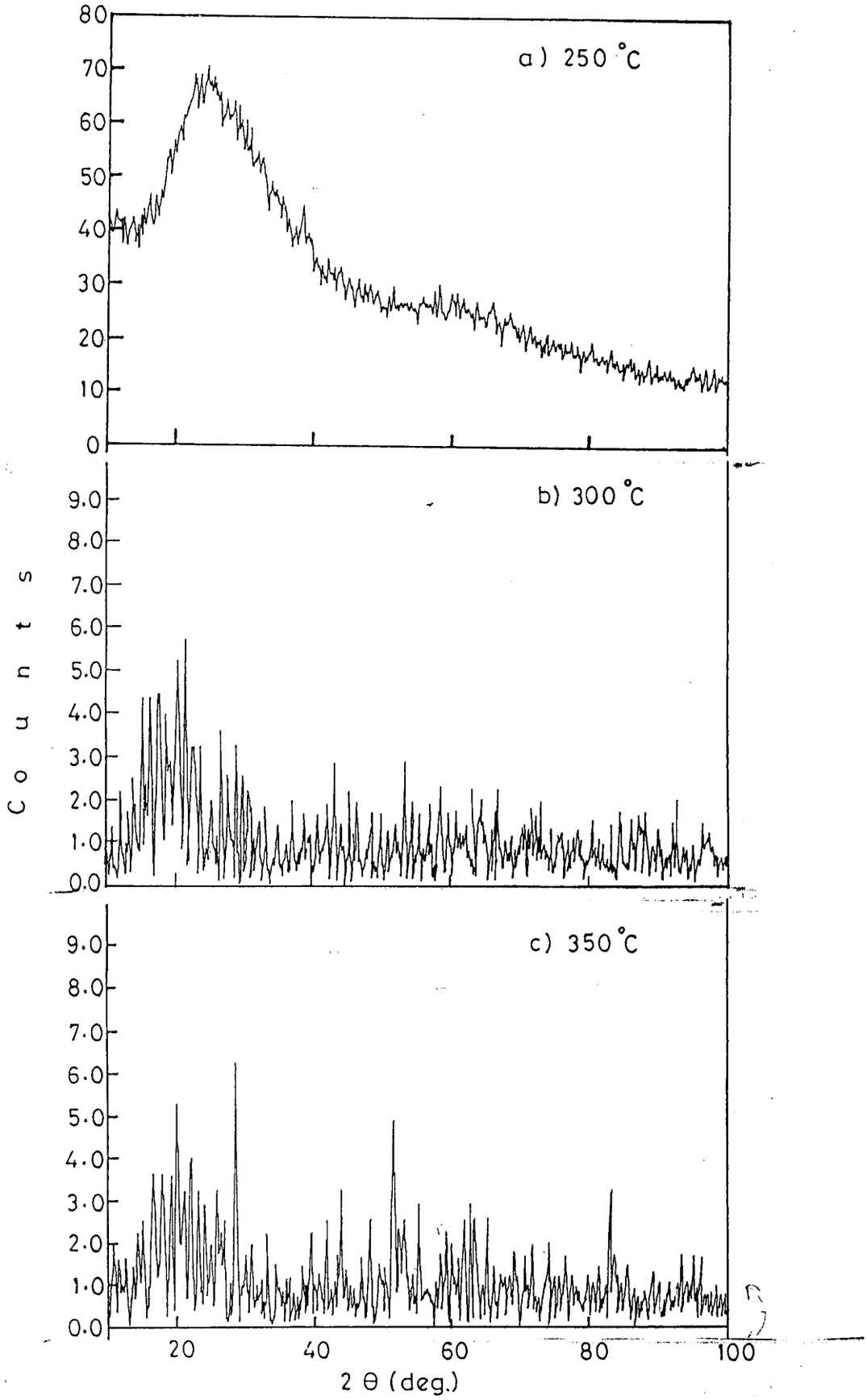

Fig.4·3 - X-ray diffraction patterns recorded for the samples deposited at (a) 250 °C (b) 300 °C and (c) 350 °C.

The 'd' values of the XRD reflections were compared with standard 'd' values from JCPDS data card [(33-0480), (80-1917)]. To diagnose the structure and composition of deposited films, JCPDS data cards were used. The observed and standard 'd' values are listed in table 4.3. The good agreement between observed and standard 'd' values suggests that at a deposition temperature of 250^0C, Cu_4O_3 phase is obtained and films deposited at 300^0C are of cubic Cu_2O phase. At the 350^0C temperature, deposited film is found to be of CuO monoclinic crystal structure.

Our XRD results are in close agreement with the reported XRD phases of copper oxide at varied deposition temperatures. It can hence be concluded that the Cu_2O phase is formed at temperature, $t \leq 300^0$C, which transforms into CuO phase above it, for all the deposition techniques, except for CVD, in which case, a mixture of Cu_2O and CuO is formed.

Table 4.3 : Comparison between observed and standard 'd' values of as deposited films

Sample	Angle 2θ	Standard 'd' values (A^0)	Observed 'd' values (A^0)	(I/I_{max}) %	Plane (hkl)	Structure
C_{250}	35.514	3.17	3.11	100.0	(112)	Cu_4O_3
C_{300}	45.89	2.46	2.44	100.0	(004)	Cu_2O
C_{350}	51.51	1.77	1.77	49.0	(112)	CuO
	54.64	1.62	1.67	28.4	(021)	CuO
	68.87	1.36	1.36	100.0	(221)	CuO
	82.94	1.16	1.16	64.0	(222)	CuO

The samples C_{250} to C_{350} were further annealed in air at 500^0C for half an hour. Figure 4.4 shows patterns of annealed films C_{A250} to C_{A350}. It is found that all the annealed samples C_{A250} to C_{A350} are of monoclinic CuO phase. The observed and standard 'd' values are listed in table 4.4. The good agreement of observed 'd' values with standard 'd' values from JCPDS data card shows formation of stable CuO phase for all the annealed samples. However, the samples deposited at 350^0C exhibit higher crystallinity than other samples, which clearly entails the role of substrate temperature on crystallinity of the copper oxide thin films.

Table 4.4 : Comparison between observed and standard 'd' values of annealed films

Sample	Angle 2θ	Standard 'd' values (A^0)	Observed 'd' values (A^0)	Plane (hkl)	Structure
C_{A250}	30.79	2.75	2.81	(110)	CuO
	30.56	2.52	2.52	(111)	CuO
C_{A300}	30.79	2.75	2.79	(110)	CuO
	35.56	2.52	2.52	(111)	CuO
C_{A350}	30.79	2.75	2.80	(110)	CuO
	35.56	2.52	2.52	(111)	CuO

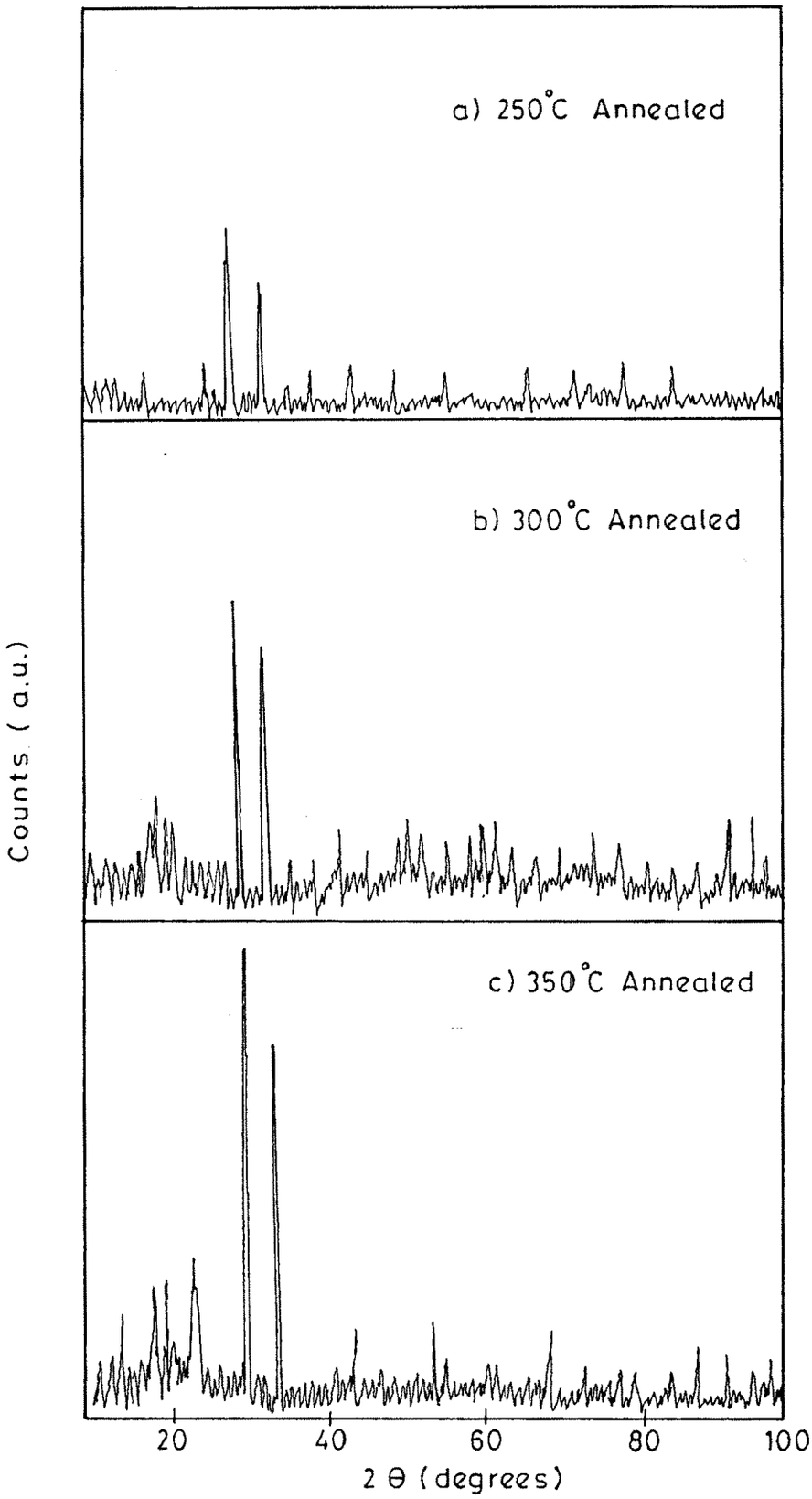

Fig. 4·4 – X-ray diffraction patterns recorded for the samples deposited at (a) 250 °C (b) 300 °C and (c) 350 °C and annealed at 300 °C for 30 minutes in air.

Copper acetate powder is annealed in air at 500^0C for 1 hour and X-ray diffraction data is obtained. XRD pattern of the annealed copper acetate powder in the range of angle 2θ between 10^0 and 100^0 is shown in figure 4.5. The observed and standard 'd' values are listed in table 4.5 indicating formation of CuO.

Table 4.5 : Comparison between observed and standard 'd' values of annealed copper acetate powder

Angle 2θ	Standard 'd' values (A^0)	Observed 'd' values (A^0)	(I/I_{max}) %	Plane (hkl)	Structure
35.71	2.52	2.51	99.5	(002), (111)	CuO
38.85	2.31	2.31	100.0	(200)	CuO
48.89	1.86	1.86	30.4	(202)	CuO
58.38	1.57	1.57	10.2	(202)	CuO
61.68	1.50	1.50	16.9	(113)	CuO
66.36	1.41	1.40	16.0	(311)	CuO
68.26	1.37	1.37	14.6	(220)	CuO

4.3.4 Optical Absorption Studies

The copper oxide thin films are optically characterized by measuring the optical density (∝t) in the wavelength range of 350 to 850 nm. The values of ∝ were not corrected for the transmittance and the reflectance of the film surface. The absorption coefficient was of the order of 10^5 cm^{-1}. In order to confirm the nature of the optical

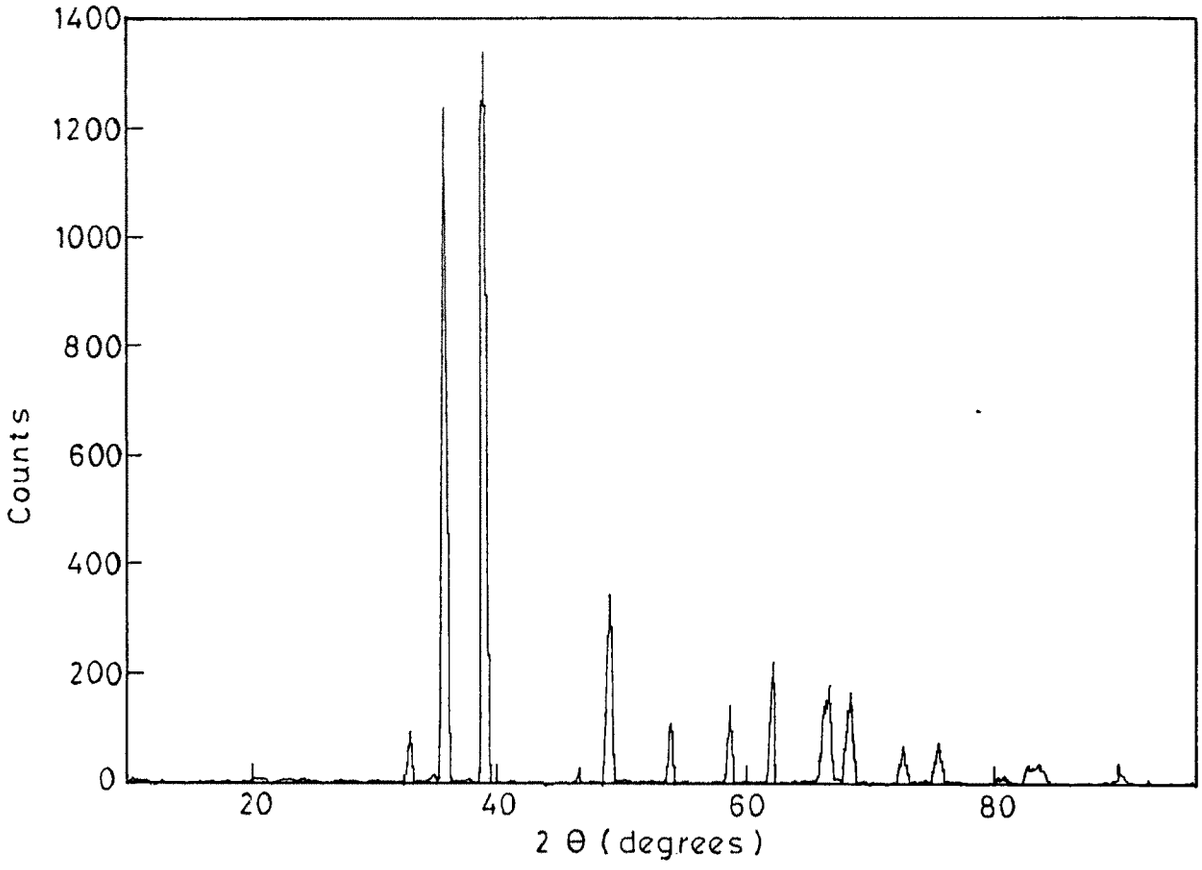

Fig.4·5- XRD of cupric acetate powder heated at 500 °C for 1 hour.

transition in these samples, the optical data were analyzed from the classical relation 3.3, for near edge optical absorption in the semiconductor.

Figures 4.6 and 4.7 show plots of $(\propto h\nu)^2$ versus $h\nu$ for the samples C_{250} to C_{350} and C_{A250} to C_{A350} respectively. Linear portion of the $(\propto h\nu)^2$ versus $h\nu$ plot indicates that optical absorption in copper oxide is due to the direct interband transition. The optical band gap energy (Eg) values were obtained by extrapolating the straight line portion of the plot at $\propto=0$. The Eg values are listed in table 4.1. It is found that band gap decreases from a value of 1.87 eV to 1.00 eV for sample C_{250} to C_{350}. After annealing the value of E_g decreases. The values of band gap of all the samples reported are in well agreement with the values obtained for copper oxide thin films deposited by activated reactive evaporation by B. R. Mehta, et al. [10]. H. H. Afify, S. S. Demian obtained E_g values of 1.4 ± 0.02 eV for sprayed CuO films on glass substrates [20]. Masaharu Fujinaka and Alexander A. Berzin reported E_g values of 2.0 eV for Cu_2O thin films deposited on glass coated with conducting film [21].

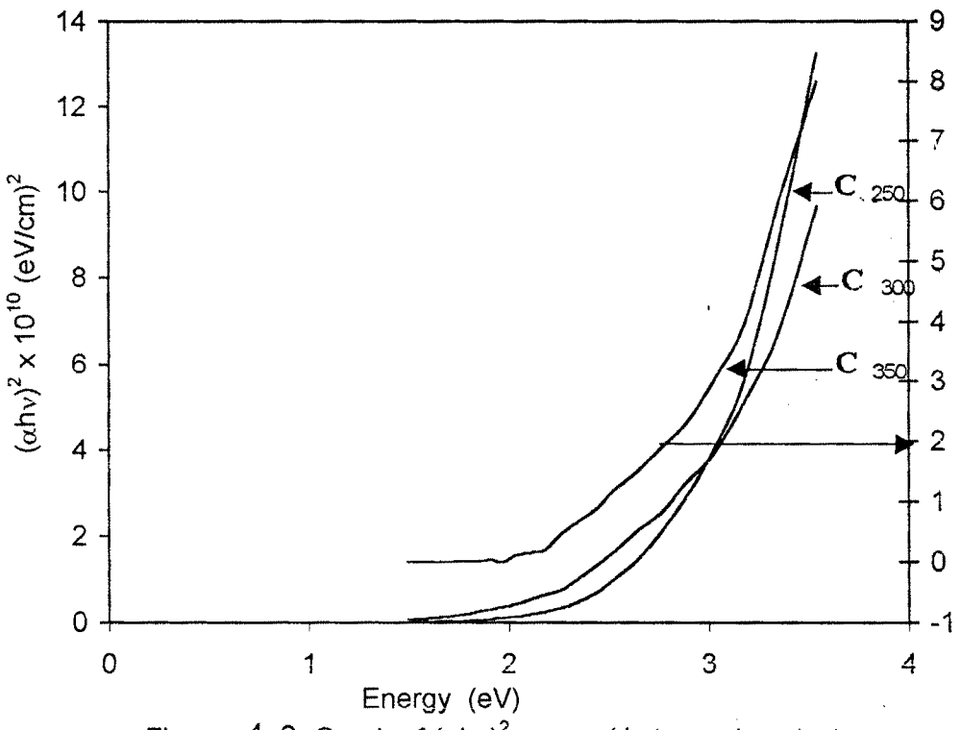

Figure 4.6 Graph of $(\alpha h\nu)^2$ versus ($h\nu$) - as-deposited samples

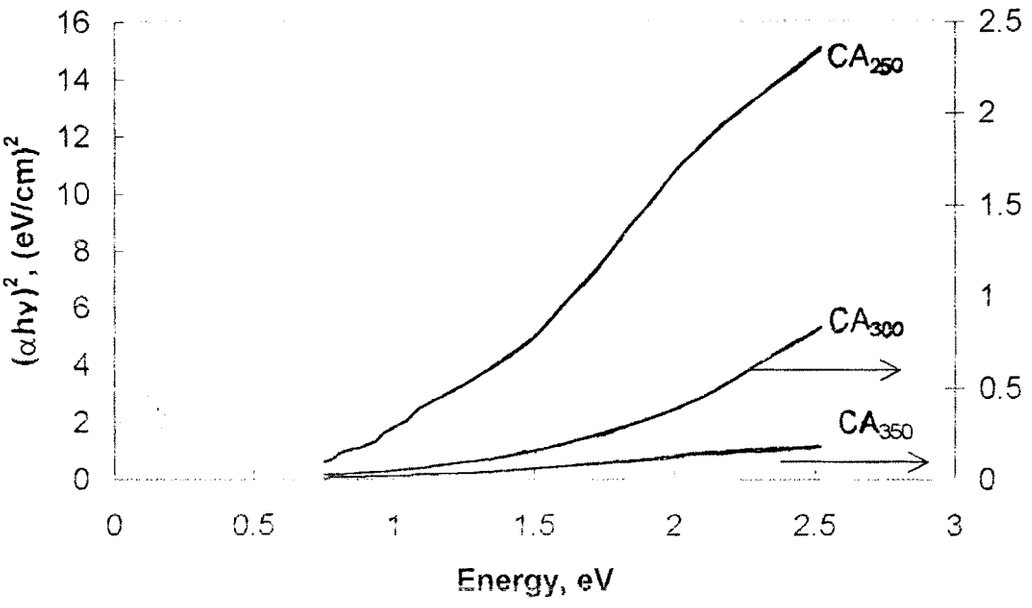

Fig 4.7 . Variation of $(\alpha h\nu)^2$ versus $(h\nu)$ for all the annealed samples.

4.3.5 Infrared Spectroscopy (IR)

Copper oxide thin film samples were studied by means of IR spectroscopy which gives information about the phase composition and the way in which oxygen is bound to the metal atoms. For infrared spectroscopic studies, copper oxide thin film samples prepared at substrate temperatures of 300^0C and 350^0C are shown in figure 4.8 (a and b). FTIR spectra for the sample C_{300} (Figure 4.8a) shows strong peak at 620 cm^{-1} corresponding to vibrational mode of Cu-O in Cu_2O phase. The infrared transmittance spectra for the sample C_{350} (Figure 4.8b) shows the absorption peaks at 416, 455, 517 and 568 cm^{-1} corresponding to CuO phase. The absence of peaks corresponding to other phases reveals that sample C_{350} has CuO phase only. The presence of only one peak at 620cm^{-1} for the sample C_{300} infer the existence of Cu_2O phase, which is in good agreement with the XRD results.

4.3.6 Electrical Resistivity

The room temperature electrical resistivity for all the samples were measured and found to vary from 10^6 Ωcm for thicker sample (C_{250}) to 10^4 Ωcm for thinner sample (C_{A350}). The room temperature electrical resistivity values for all the samples are listed in table 4.1.

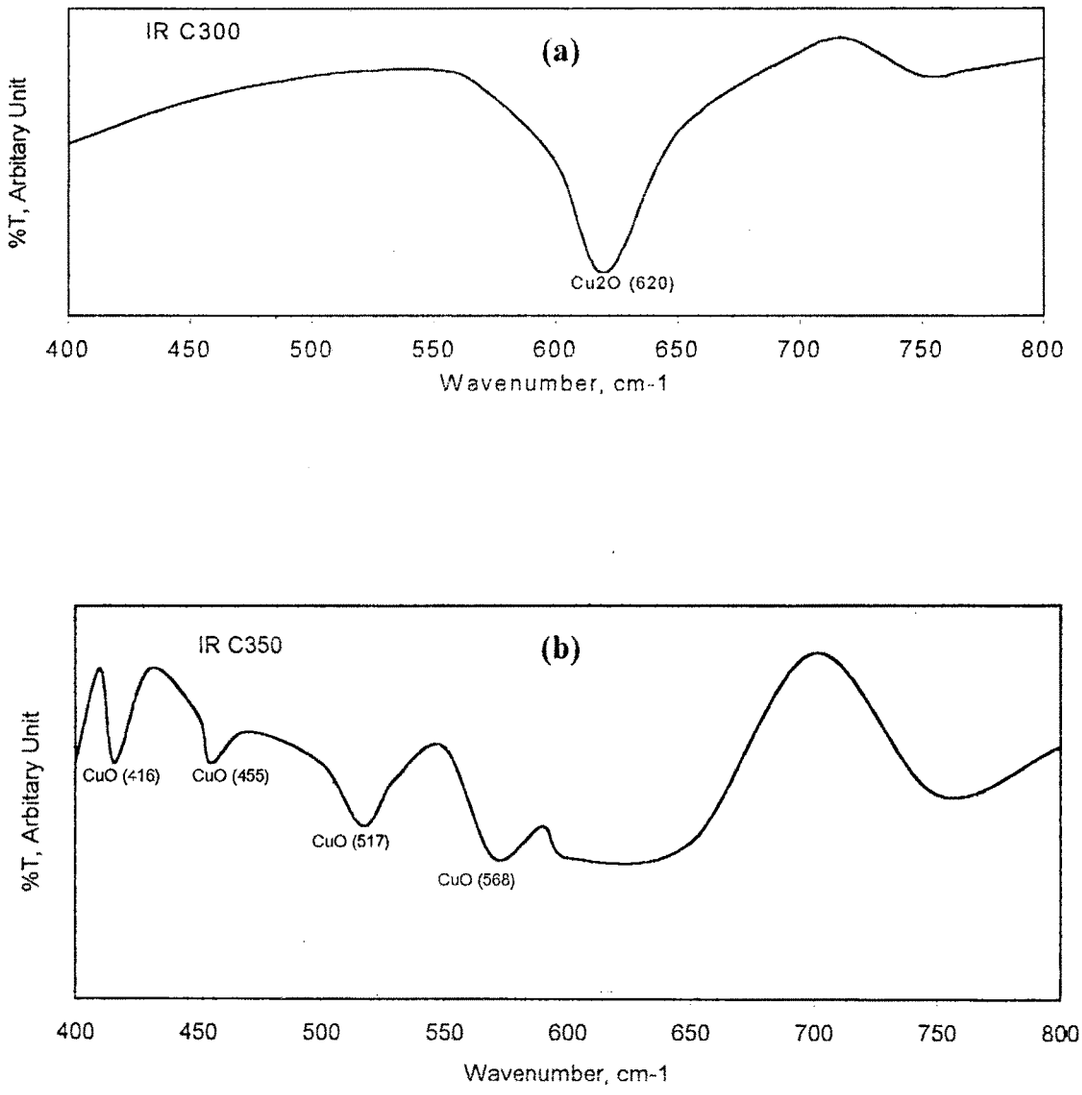

Figure 4.8 (a & b). The IR spectrum of the samples C_{300} and C_{350} respectively.

For all the samples as temperature rises resistivity decreases indicating that the films are semiconducting in nature. The thermal activation energy values (E_a) were calculated by using the relation (3-4). These values are listed in table 4.1. the calculated values of activation energy for samples C_{250} to C_{350} and for samples C_{A250} to C_{A350} are in well agreement with the reported values. Tsuyoshi Kosugi and Shoji Kaneko estimated activation energy of 0.30 eV for cuprous oxide thin films deposited by spray-pyrolysis [22]. In case of the oxides, the activation energy is the thermal energy required to hop the charges from one site to another. Figures 4.9 and 4.10 show the variation of logρ versus 1/T for C_{250} to C_{350} and C_{A250} to C_{A350} samples respectively. These plots yield straight lines, which suggest that the temperature dependence of electrical resistivity is consistent with the relation 3.5.

4.3.7 Thermo-electric Power Measurement

The temperature difference causes transport of carriers from hot end to cold end, thus creating an electric field, which gives rise to the thermal voltage. Thermo electric emf was measured for C_{250} sample in the temperature range 300 to 450K. the polarity of the thermally generated voltage at the hot end was negative indicating that the films are of p-type. Tsuyoshi Kosugi reported p-type conductivity in spray pyrolysis deposited Cu_2O films on glass substrates [22].

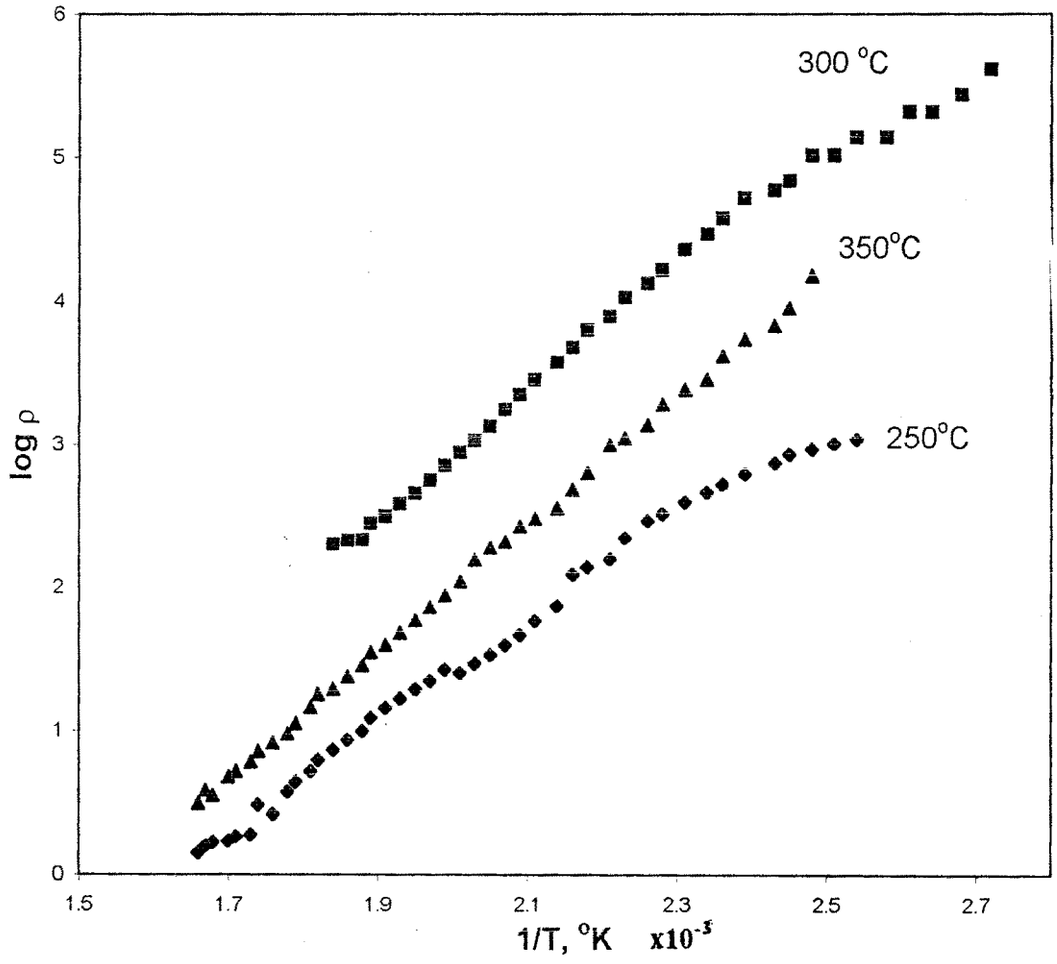

Fig. 4.9 Log ρ versus 1/T for all the as-deposited samples.

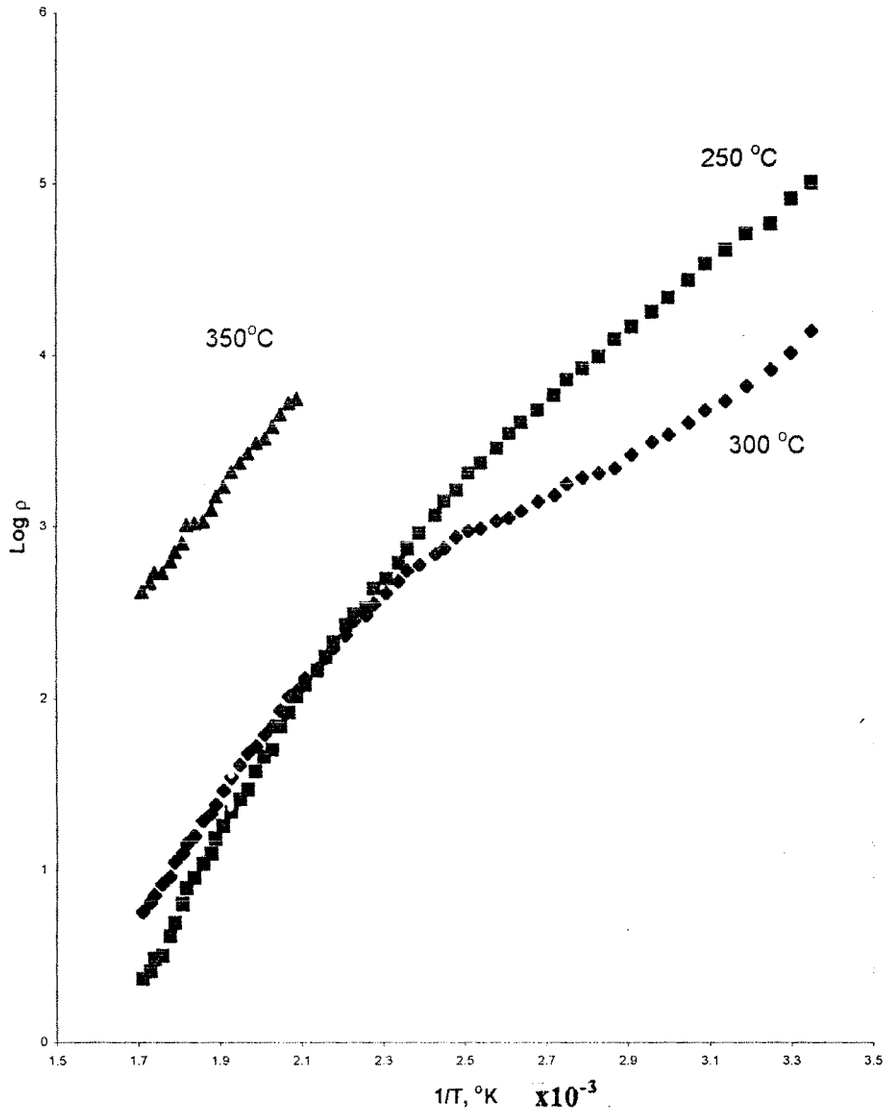

Fig 4.10 Variation of log ρ versus 1/T for all the annealed samples.

Nanocrystalline CuO films prepared by activated reactive sputtering by B. Balamurugan showed p-type conductivity [10]. F. P. Koffyberg and F. A. Benko detected p-type conductivity in all the samples, with an average thermoelectric power of 770 μV/K prepared by thoroughly grinding CuO powder moistened with the appropriate quantity of $LiNO_3$ solution. Figure 4.11 shows the variation of thermo-emf with temperature difference for C_{250} sample. The thermoelectric power for the sample C_{250} was calculated from the experimental data and is of about 0.01 mV/K. Similar results for samples C_{300} and C_{350} were obtained indicating p-type conductivity in copper oxide thin film samples.

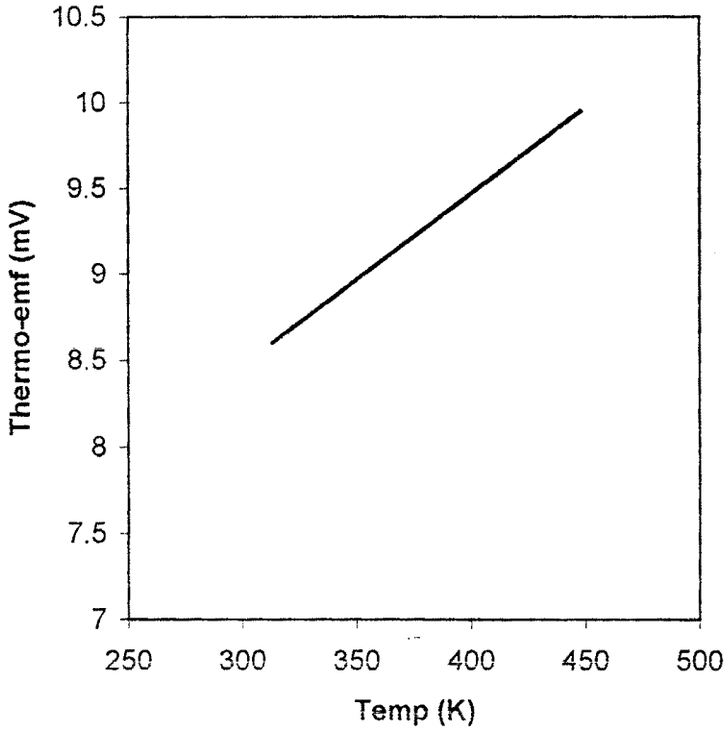

Figure 4.11Variation of thermoemf with tmeperature difference for C_{250} sample.

4.4 CONCLUSIONS

Copper oxide thin films were deposited onto the amorphous glass substrates at various substrate temperatures from 250 to 350^{0}C in the interval of 50^{0}C, using spray pyrolysis technique. The film thickness decreases from 0.131 μm to 0.045 μm as substrate temperature varied from 250 to 350^{0}C. XRD studies showed that the films deposited at 250^{0}C are amorphous while the films deposited at 300 and 350^{0}C show slight crystallinity.

The optical absorption analysis suggested the presence of direct inter-band transitions. The optical band gap decreases with increase in substrate temperature. The room temperature electrical resistivity varies from 10^6 Ωcm to 10^4 Ωcm with increase in substrate temperature from 250 to 350^{0}C, showing p-type semiconductivity.

An interesting result was obtained when films were annealed at 500^{0}C for half an hour. XRD studies showed that the annealed films were polycrystalline consisting copper oxide (CuO) monoclinic phase. Thickness, electrical resistivity and band gap of the annealed films decrease. Therefore, it is concluded that the material properties can be tailored merely by changing the substrate temperature.

4.5 REFERENCES

1. T. J. Richardson, J. L. Slack, M. D. Rubin, Electrochimica Acta, 46 (2001), 2281.

3. S. Santra, C. K. Sarkar, M. K. Mukherjee, B. Ghosh, Thin solid Films 213 (1992) 226.

3. R. Padyath, J. Seth, S. V. Babu, Thin solid Films 239 (1994) 8.

4. K. H. Yoon, W. J. Choi, D. H. Kang, Thin Solid Films, 372 (2000).

5. P. Luzeau, X. Z. Xu, M. Lagues, N. Hess, J. P. Contour, M. Nanot, F. Queyroux, M. Touzeau, D. Pagnon, J. Vac. Sci. Technol., A8 (1990) 3938.

6. E. Fortin, D. Masson, Solid State Electron., 25 (1982) 281.

7. W. M. Sears, E. Fortin, Solar Energy Mater., 10(1984) 93.

8. J. Harion, E. A. Niekish, G. Schari, Solar Energy Mater., 4 (1980) 101.

9. L. Papadimittriou, N. A. Economou, D. Trivich, Solar Cells, 3 (1981) 73.

10. B. Balamurugan, B. R. Mehta, Thin Solid Films, 396 (2001) 90.

11. L. W. Chow, Y. C. Lei and H. L. Lowk, Thin Solid Films, 81 (1981) 3706.

12. M. D. Uplane and S. H. Pawar, Solid State Comm. 46 (1983) 847.

13. S. H. Pawar, S. P. Tamhankar and C. D. Lokhande, J. Mat. Sci. Lett. 3 (1984) 427.

14. S. Kaneko, T. Kosugi, Ti Fujiwara and M. Okuya, Proceedings of the symposium on Photovoltaics for 21st century of the Electrochemical Society (1999).

15. V. F. Drobny and D. L. pulfrey, Thin Solid Films, 61 (1979) 89.

16. T. Maruyama, Jpn. J. Appl. Phy. 37 (1998) 4099.

17. O'Nell P. Ignatier A. and Doland C., Solar Energy, 21 (1978) 465.

18. Rakhashani A. E., Solid State Electron., 29 (1986) 7.

19. Mentero C., Poillerat G. and Meas Y., Thin Solid Films, 19 (1989) 353.

20. H. H. Afify, S. E. Demian, M. A. Helal and F. A. Mahmood, Indian Journal of Pure and Applied Phy., 37 (1999) 379.

21. M. Fujinaka and A. A. Berezin, J. Appl. Phys., 54 (1983) 3582.

22. Tsuyoshi Kosugi and Shoji Kaneko, J. Am. Ceram. Soc., 81 (1998) 3117.